Jacob W. Albrecht
Klavs F. Jensen

Department of Chemical Engineering,
Massachusetts Institute of Technology,
Cambridge, MA, USA

Received July 13, 2006
Revised August 14, 2006
Accepted August 18, 2006

Research Article

Micro free-flow IEF enhanced by active cooling and functionalized gels

Rapid free-flow IEF is achieved in a microfluidic device by separating the electrodes from the focusing region with porous buffer regions. Moving the electrodes outside enables the use of large electric fields without the detrimental effects of bubble formation in the active region. The anode and cathode porous buffer regions, which are formed by acrylamide functionalized with immobilized pH groups, allow ion transport while providing buffering capacity. Thermoelectric cooling mitigates the effects of Joule heating on sample focusing at high field strengths (~500 V/cm). This localized cooling was observed to increase device performance. Rapid focusing of low-molecular-weight p*I* markers and Protein G–mouse IgG complexes demonstrate the versatility of the technique. Simulations provide insight into and predict device performance based on a well-defined sample composition.

Keywords: Free-flow IEF / Microfabrication / Protein separation
DOI 10.1002/elps.200600436

1 Introduction

As a separation technique, IEF is used to sort and concentrate a sample into subfractions based on p*I*. IEF also has the advantage of acting orthogonally to size-based separations (*e.g.*, SDS-PAGE), making it very attractive for low-resolution prefractionation and concentration. However, IEF in a gel, as it is most commonly used, requires several hours of focusing at high voltages. Microscale IEF has been shown to operate much more quickly [1–6], making micro-IEF devices desirable tools in simplifying complex biological samples for enhancing the sensitivity of subsequent detection assays. Unfortunately, the processing of biologically relevant sample volumes (~100 μL) remains a challenge for microfabricated batch separation techniques.

Free-flow electrophoresis (FFE) [7, 8] works by applying an electric field perpendicular to a sample as it flows through a rectangular channel. With FFE, continuous operation allows sample volumes much larger than the device operating volume to be fractionated and collected. IEF is an ideal mode of electrophoresis for use in FFE as it concentrates species as they are focused to their p*I*. In this way, sample complexity can be reduced without losses associated with dilution. Losses associated with nonspecific adhesion can be mitigated by using a large sample volume relative to the device surface area, reducing the importance of surface passivation. Also, a wide, open sample channel increases the tolerance for complex biological samples, as organelles [9] and protein aggregates can be focused in the device without clogging.

There are technical challenges in constructing these devices due to the relatively large amount of electrical energy that must be delivered to the focusing sample. The primary barrier is in applying voltages high enough to create the electric field strengths needed for focusing. With the sample in direct contact with metal electrodes [3, 9], electrolysis of water creates bubbles in the channel when voltages above ~3 V are applied. Recently, several groups have devised designs to surmount this barrier by isolating the metal electrodes. Fabricated wells [10, 11] above an IPG gel have been used to fractionate samples. For microfabricated channels, a fabricated array of channels with high hydrodynamic resistance [5, 12–15] served as the electrical interface for the sample channel. Hydrogel channels formed by casting agarose around a nylon filament were

Correspondence: Professor Klavs F. Jensen, Department of Chemical Engineering, Massachusetts Institute of Technology, Cambridge, MA 02139, USA
E-mail: kfjensen@mit.edu
Fax: +1-617-258-8224

Abbreviations: APS, ammonium persulfate; **FFE**, free-flow electrophoresis; **HPMC**, hydroxypropylmethylcellulose

shown to allow transverse electric fields of 5–10 V/cm [16]. Kohlheyer *et al.* [2] used photopolymerized acrylamide within a glass device as an ion bridge, in conjunction with buffer sheath flows, to perform rapid IEF and zone electrophoresis.

A second challenge to device performance is Joule heating of the sample when large voltages are applied. Typically, conventional IEF uses active cooling to counteract heating effects, while microscale devices have relied on the high heat transfer inherent to microdevices to keep the sample at reasonable operating temperatures. However, assuming isothermal operation is not necessarily true for microsystems with high-applied voltages. Because Joule heating increases roughly with the voltage squared, higher applied voltages require much more heat dissipation, perhaps more than what is possible by natural convective cooling to the environment. Models for Joule heating in microfluidic channels [17] have explored the effect of insulating material as well as autothermal (runaway) liquid heating.

Here, we design and test a device to perform free flow IEF. Our approach involves fabricating thin gel slabs within a PDMS device, not only as structural material, but also as a chemically significant part of the device. Our design motivations were to improve upon previous work [2, 3, 5, 9] not necessarily in terms of resolution, but in terms of allowing for nonideal samples, lowering hydraulic resistance, and simplifying fabrication and operation. Heat transfer from the device is also a key concern; active heat transfer should be employed to prevent overheating of the device at high-applied voltages.

2 Materials and methods

2.1 Design and fabrication

The free-flow IEF device (Fig. 1) was designed to have a sample channel defined by a porous material capable of allowing ion conduction between the sample channel and the electrode buffer, while preventing unwanted fluid convection between the two regions. The porous material should ideally have no EOF as well as very small pores to facilitate ion conduction. Other characteristics, such as good mechanical strength and inertness were desired to improve device durability. The design was based on a PDMS channel bordered by posts to define placement of the porous material without the need for a photo-polymerization mask. The need for a high degree of anisotropy in the device (tall posts around a rectangular sample channel) as well as the height of the sample channel led to the fabrication of the device in PDMS. Small liquid reservoirs were located on either side of the device containing catholyte and anolyte as well as platinum electrodes which were connected to an external power source.

The bulk of the device was fabricated using standard soft lithography techniques [18]. Briefly, a silicon wafer was coated with a layer of SU-8 2050 (MicroChem, Newton, MA, USA), which was pattered using a 5080 dpi transparency mask (Pageworks, Cambridge, MA, USA). Next, Sylgard 184 (Dow Chemicals, Midland, MI, USA) was cast over the SU-8 mold and cured at 70°C for 2 h. After curing, the PDMS was peeled off of the master; individual devices were cut out, and fluidic connections were punched using a 20 gauge Luer stub adapter (Becton-Dickinson, Sparks, MD, USA). When a 23 gauge Luer stub adapter was inserted in to these holes, the connection was self-sealing; no epoxy or glue was necessary. Next, the devices were treated with oxygen plasma for 40 s prior to permanently bonding to a 25 mm $\times$ 40 mm glass cover-slip (VWR, West Chester, PA, USA).

2.2 Gel casting

The gel was cast inside the device on each side of the sample channel (Fig. 1) after the PDMS had been sealed to the glass substrate. In order to ensure that the PDMS surfaces regained their hydrophobicity following the plasma treatment, there was a 24 h wait before gel casting. Surface tension effects at the poststructures (Fig. 1b) confined the gel and prevented penetration into the sample channel during casting.

Polyacrylamide has been used in other microfluidic applications [1, 2, 19, 20] and is usually patterned by UV initiated polymerization. The present device was designed to avoid this step. In this case, ammonium persulfate (APS; VWR) was used as the free radial initiator. Since oxygen inhibits acrylamide polymerization and has a high permeability in PDMS [21], thorough oxygen removal procedures were required. To remove oxygen, the PDMS devices were placed in a vacuum oven at 70°C and 50 mmHg for more than 8 h. Subsequently, the devices were kept under nitrogen. The monomer solution used in the polyacrylamide devices tested was 15% total acrylamide (15% T), with 3% of the acrylamide present as *bis*-acrylamide (3% C) (PlusOne ReadySol IEF, GE Healthcare, Piscataway, NJ, USA). Solutions containing acrylamide are neurotoxic and should be handled with caution. Immobilines (pK_a 3.6 and 9.3, GE Healthcare) were added to the monomer solution to a final concentration of 12 mM. For the anode side gel, 1 mL of this monomer solution was mixed with 80 μL of 1% v/v Triton X-100 (EMD Chemicals, Gibbstown, NJ, USA), 3 μL of 1 M Na_2SO_3, 3 μL of 1 M $Na_2S_2O_5$ (Mallinckrodt Baker,

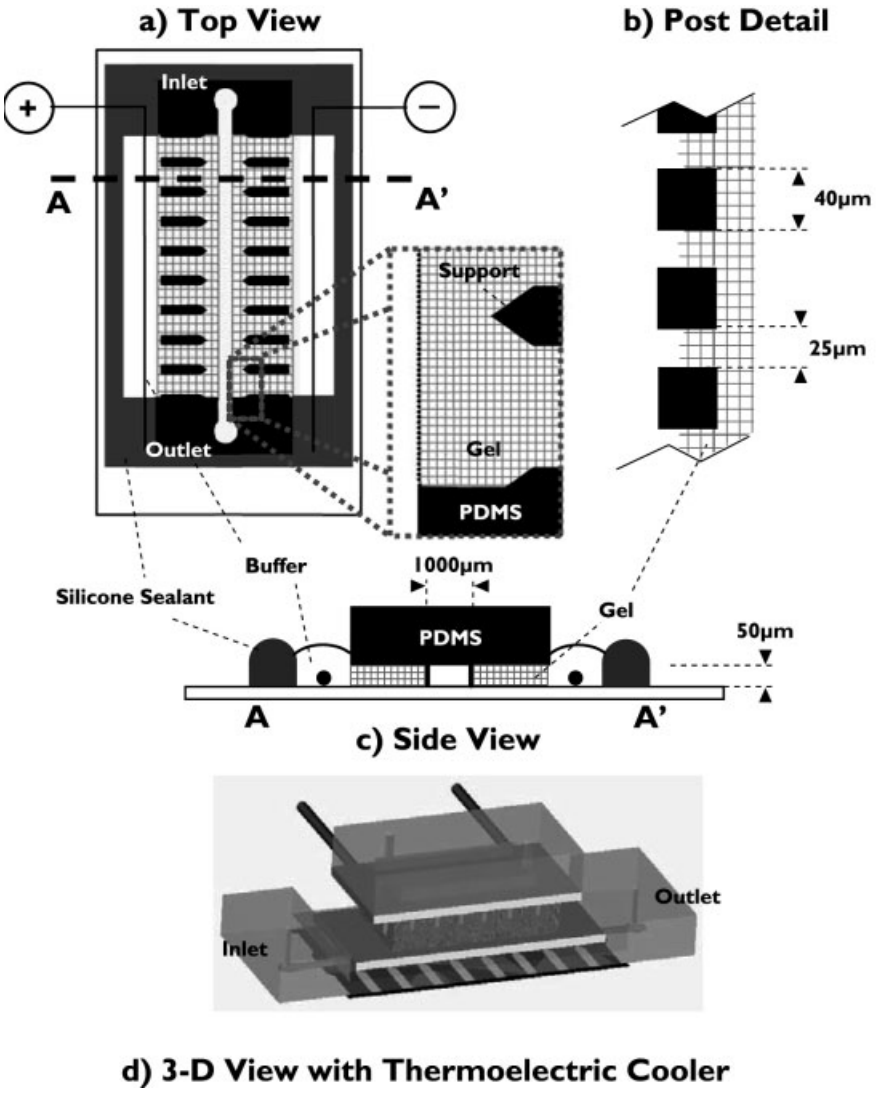

Figure 1. Layout of transverse IEF device. Top view (a) shows the PDMS device with the sample channel bordered by left and right porous material regions (cross-hatched areas) and anode and cathode, respectively. Silicone sealant (solid gray) is used to form the reservoirs for the anolyte and catholyte buffers, as well as to hold the platinum electrodes in place. The sample channel is 1 mm wide, 20 mm long, and 50 μm deep. It is separated from the gel sections by 40 μm × 40 μm, 50 μm tall posts (b) spaced 25 μm apart (307 posts on each side of the channel). Larger elongated poststructures (0.75 mm × 3 mm rectangle with 0.75 mm equilateral triangle) support the fragile postarray and the porous regions. The device presented has a single inlet and single outlet. Side view (c) shows the device in cross-section (not to scale). A rendering of the device with a thermoelectric cooler (d) illustrates the placement of the cooling module, heat spreaders, and water-cooled chip.

Phillipsburg, NJ, USA), 2 μL of 230 mM $CoBr_2$ (Sigma-Aldrich, St. Louis, MO, USA), 2 μL TEMED (EMD Chemicals), and 6 μL of 10% APS (EMD Chemicals), in this order. The cathode side gel had a slightly different recipe, the proportion was 1000:40:3:3:2:1:6, for the reagents, respectively. There were two reasons for the different recipes: (i) the cathode gel mixture had a lower surface tension due to the pK_a 9.3 Immobiline, so less Triton was necessary and (ii) only the basic form of TEMED accelerates polymerization, so more is needed for low pH gels. Cobalt, sulfite, and metabisulfite levels were adjusted to scavenge oxygen quickly [22]. After adding APS as the initiator and TEMED as the polymerization accelerator, the liquid mixture was introduced to the side of the device, where it was drawn in by capillary action. Surface tension held the monomer solution at the postarray, long enough for the gel mixture to become crosslinked; approximately 40 s.

2.3 Device packaging and operation

Platinum wires (0.5 mm diameter, Alfa Asear, Ward Hill, MA, USA) were used to connect the electrode reservoirs to a high-voltage electrophoresis power supply (VWR). Silicone sealant (ASI 502, American Sealants, Fort Wayne, IN, USA) was used to fix the wires in place and to form reservoirs for the anolyte and catholyte buffers. The anolyte used was 20 mM phosphoric acid with 0.4% w/v hydroxypropylmethylcellulose (HPMC, Fluka, Buchs, Switzerland); the catholyte was 20 mM lysine and 20 mM arginine (1 × IEF Cathode Buffer, BioRad, Hercules, CA, USA) in 0.4% HPMC. To reduce protein adsorption and EOF [23], the channel was incubated with a 1% w/v solution of poly(vinyl alcohol) (PVA, MW 146–186 kDa, 87–89% hydrolyzed, Sigma-Aldrich) at room temperature overnight. Sample buffers were pulled through the device using a syringe pump (EW-74901-10, Cole-Parmer, Ver-

non Hills, IL, USA) set to withdrawal mode. At the inlet of device, a 200 μL pipette tip was simply inserted into the PDMS. This sample reservoir was easily refilled by pipetting samples onto the top of the pipette tip. Different samples could also be "queued" by using 10 μL of perfluorodecalin (Sigma-Aldrich) as a spacer. The negative pressure applied to the outlet of the device was sufficient to ensure steady operation without adversely affecting the polyacrylamide gel. In separate trials, to ensure that there was no fluid convection through the gel, a suspension of fluorescent beads flowing through the device (6 μm, Duke Scientific, Palo Alto, CA, USA) without an applied voltage was not observed to focus hydrodynamically or to slow as they moved down the sample channel.

Joule heating was counteracted by active cooling with a miniature thermoelectric cooler (TE-35-0.6-1.0, TE Technology, Traverse City, MI, USA) placed on top of the device. Although cooling through the PDMS side of the device is much less efficient (the thermal resistance is roughly 60 times greater than the glass coverslip), it was necessary in order to observe focusing within the device. The cold side of the TE module was separated from the focusing channel by a 0.6 mm thick silicon heat spreader and 1 mm thick layer of PDMS. The hot side of the TE device was cooled by water flowing through a custom made PDMS and silicon chip. To assemble these chips, PDMS was cured around a small piece of glass (approximately 5 mm × 13 mm × 1 mm high) to create a rectangular chamber. After curing, the PDMS was cut to the size of the silicon heat sink (approximately 8 mm × 20 mm × 4 mm high) and fluidic connections were punched out on opposite corners of the chamber. The PDMS and silicon chip were treated with oxygen plasma for 1 min to ensure adequate bonding. The cooling rate of the TE module was adjusted by varying the water flow rate through the PDMS and silicon chip (1–3 mL/min). This sealed chip was affixed to the top (hot side) of the TE module with a thermal joint compound (Type 120, Wakefield Engineering, Pelham, NH, USA) and 5-min epoxy (Devcon, Danvers, MA, USA). A separate power supply (Protek 3015B, Tempe, AZ, USA) was used to supply 3 V and 0.75 A to the module. The cooling rate at this amperage was measured to be between 0.35 and 0.88 W, depending on the water flow rate used.

2.4 Dye and protein preparation

Dye focusing experiments were conducted with fluorescent low-molecular-weight p*I* markers (p*I*: 3.5, 5.1, 7.2, 7.6, and 9.5, Fluka, Buchs, Switzerland) and fluorescein disodium salt (EMD Chemicals). Markers were used at a final concentration of 1 mg/mL and a final fluorescein concentration of 13.3 μM was used. In all cases, Ampholine 3–10 was mixed to a final concentration of 2% in deionized water (Millipore, Billerica, MA, USA). To reduce EOF and increase solubility, HPMC and Triton were added to final concentrations of 0.2% w/v and 0.1% v/v, respectively.

For protein focusing experiments, FITC BSA (Sigma-Aldrich) was used at 130 μg/mL (~2 μM) in 2% Ampholine 3–10, and with 0.2% w/v HPMC in deionized water. Because of the low ionic strength and BSAs proclivity for nonspecific adhesion, Triton was used at a final concentration of 0.5% v/v. For affinity IEF experiments, Alexa 488 conjugated Protein G (Invitrogen, Carlsbad, CA, USA) and chromatographically purified Mouse IgG (Invitrogen) were mixed in PBS (Invitrogen). For all experiments, the concentration of Protein G was held constant at 20 μg/mL (1 mM). To remove any free dye in solution, 0.5 mL of Protein G (20 μg/mL) was dialyzed using a dialysis cassette (Slide-A-Lyzer 3500 MWCO, Pierce Biotechnology, Rockford, IL, USA) in 500 mL of PBS for 16 h. Ampholine 3–10 was added to a final concentration of 2% prior to the addition of IgG. The mixture was allowed to react for a minimum of 15 min prior to focusing. For pure Protein G and low levels of IgG (5 μg/mL), no Triton or HPMC was added to the mixture. For high levels of IgG (22 μg/mL), Triton was added to 0.1% v/v to reduce agglomeration and precipitation at the complex's p*I*. In the event of excessive precipitation at high levels of IgG, the device was flushed with 100 μL of 1% Triton to remove adsorbed protein.

2.5 Current measurements

Current measurements were made with a digital multimeter (NI-4060) and LabView software from National Instruments (Austin, TX, USA). To measure total current, a 100 Ω current shunt was used, with the corresponding voltage drop measured by LabView. From these measurements, changes in sample conductivity due to IEF and Joule heating could be approximated. Once applied, the total current varied as a function of time, dropping as the buffer regions equilibrated and the ampholytes in the sample became focused.

2.6 Imaging and analysis

Focusing behavior was observed with an inverted fluorescent microscope (Axiovert 200, Carl Zeiss, Thornwood, NY, USA) with a high speed 8-bit color camera (MF-046C, Allied vision technology). A near-UV excitation filter was employed in p*I* marker focusing, and a FITC filter

(green channel) was used to detect green fluorescence. Full frames were captured with a shutter time between 100 ms and 2.5 s, depending on the fluorescent intensity of the sample. The images captured by the camera were subsequently processed by programs written in MATLAB (The Mathworks, Natick, MA, USA). Full-color images were desaturated prior to analysis. To find pixel intensity across the width of the channel, 100–500 pixels from a steady state image were averaged and normalized to the maximum intensity.

2.7 Simulation of species in an idealized ampholyte buffer

For simplicity, the steady-state 2-D focusing in the device may be approximated as a transient 1-D problem. A 1-D free-flow IEF model was developed similar to Bier *et al.* [24–26]. Briefly, for an idealized ionic species undergoing electrophoresis, the general time-dependent 1-D formulation is given by the following system of equations:

$$\frac{\partial C_i}{\partial t} = \frac{\partial}{\partial x}\left(D_i \frac{\partial C_i}{\partial x} - \mathbf{E}\frac{z_i D_i F}{RT} C_i\right) \quad (1)$$

$$J = -E\frac{F^2}{RT}\sum_i z_i^2 D_i C_i - F\sum_i z_i D_i \frac{\partial C_i}{\partial x} \quad (2)$$

$$\left[H^+\right] - \frac{K_w}{\left[H^+\right]} + \sum_i (z_i C_i) = 0 \quad (3)$$

Equation (1) describes the species concentration, C_i, as a function of both position and time. Here, C_i depends on the diffusion constant, D_i, charge number, z_i, temperature, T, and the local electric field, **E**. Equation (2) is the current density within the device, assuming no ionic convection. Equation (3) enforces electroneutrality, which is assumed in the sample channel, where K_w is the dissociation constant for water. In Eqs. (1) and (2), F is Faraday's constant and R is the ideal gas constant. The integral of the electric field was set equal to the applied voltage. In the case of IEF, the sign of z_i changes as the species enters regions of different pH, reversing the electrophoretic flux at the p*I*. From Eq. (1), it is apparent that the performance of IEF depends on both the diffusive and electrophoretic fluxes of the sample. The second term in Eq. (2) describes the current density due to the diffusive flux of ions in the sample buffer. In order to simplify the system of equations; this diffusive current was assumed to be negligible compared to the current due to the applied field. To validate the model, previously published results [24, 25] were reproduced.

To model the formation of the pH gradient, the model considered phosphate ions (0, −1, and −2 valences), sodium ions, fluorescein as well as 150 theoretical ampholytes. These ampholytes were assumed to be biprotic with p*I*'s uniformly spanning the range of 3–10. The difference between the lower pK_a and higher pK_a was set to be 2 pH units [26]. Focusing of BSA was simulated with a protein model similar to Mosher *et al.* [27, 28]. However, BSA titration data [29] were made continuous by a quartic/cubic rational fit. The system of equations used in the model constitutes a set of differential-algebraic equations (DAEs), which were integrated numerically by DAE software (Jacobian, Numerica Technologies, Cambridge, MA, USA).

3 Results and discussion

3.1 Model evaluation and device characterization

It is useful to identify the electric fields present in the sample channel *versus* the gel. By rapidly replacing the sample solution of solution with a high, known conductivity (1 M KCl), the resistance due to the regions outside the sample channel can be estimated. Depending on the original conductivity of the sample introduced to the device, the gel (which accounts for ~90% of the cross-sectional area) was measured to have a lower average electric field than the focusing sample. For samples with high conductivity, *i.e.*, containing PBS, the electric field in the gel was determined to be 4.7 times lower than in the sample channel, presumably due to salt taken up by the gels. For the case of fluorescent IEF markers, which were dissolved in deionized water and 2% Ampholine, the electric field in the gel was half that in the sample channel.

To demonstrate IEF and modeling of proteins, FITC-conjugated BSA (FITC-BSA) was selected. BSA has a well-known titration profile [29], with a p*I* of approximately 4.8. Figure 2a shows the simulated and actual focusing of FTIC-labeled BSA. The field strength was estimated to be 500 V/cm, with focusing completed less than 72 s. Despite the high level of surfactant, there was some adhesion of FITC-BSA at the anode and at its p*I*. There was also a second, unknown peak that appeared at a more neutral pH, most likely an impurity or protein degradation product. Nonetheless, there was good agreement of simulation and experiment, both in the location of the focusing as well as peak width.

Another method of observing the pH gradient formed in the device is to use pH dependent fluorescent indicators such as fluorescein. Fluorescein has four relevant charge states: −2, −1, 0, and +1, that have different fluorescent properties. Fluorescein's pH behavior is well known and can be used to identify pH gradients. In IEF, a change in fluorescent intensity will identify the pH across the width

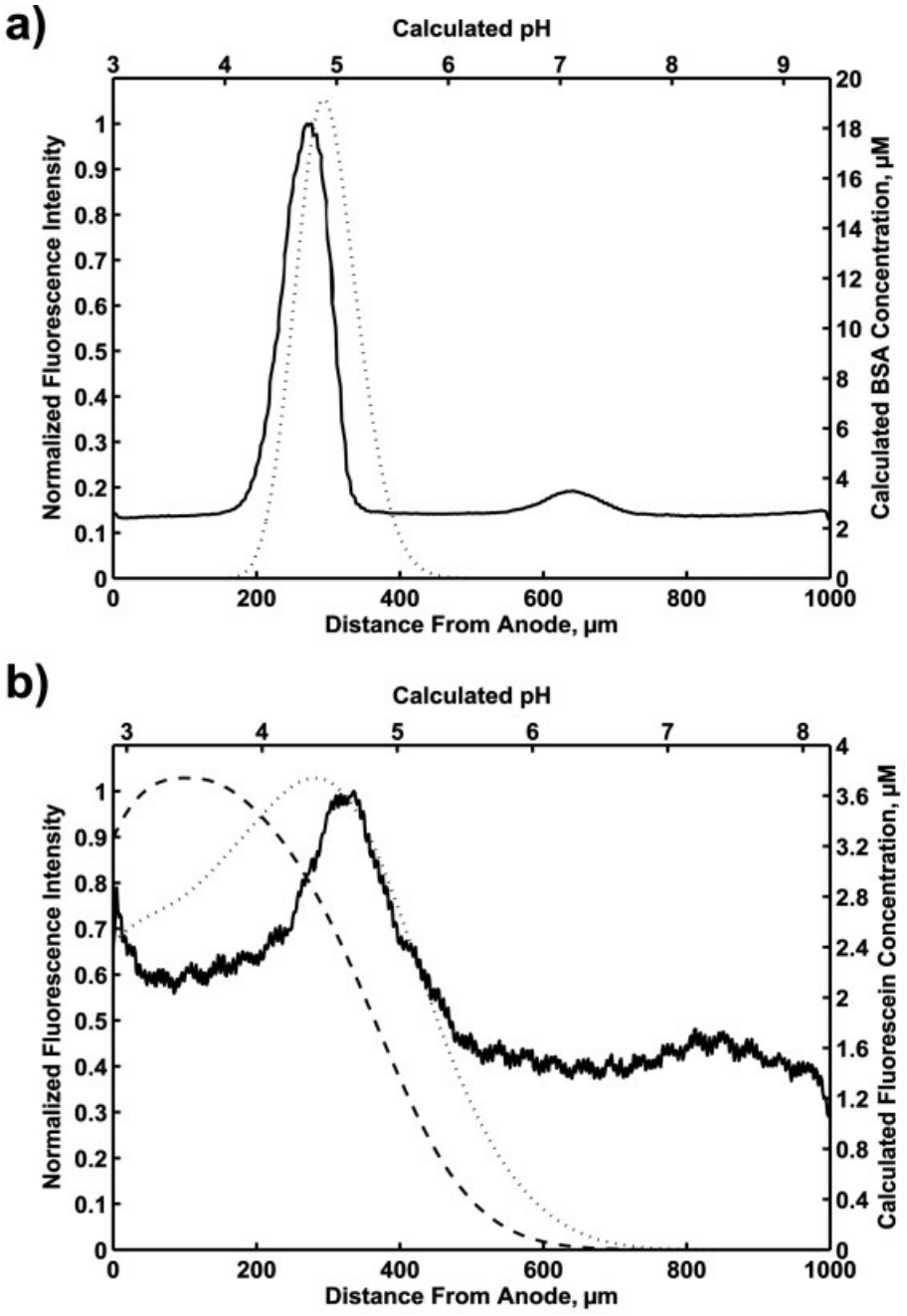

Figure 2. Comparison of experimental results to theory. (a) Focusing of FITC-tagged BSA and comparison to theoretical behavior. Solid line indicates fluorescent intensity across channel after a 72 s residence time and an applied voltage of 150 V. The dashed line is the calculated steady state focusing profile for an average field strength of 500 V/cm. Also, a secondary focusing band, presumably an impurity or a degradation product of the protein, is at pH ~7.5. (b) Focusing of fluorescein. Solid line shows the measured normalized fluorescent intensity across channel after a 36 s residence time and an applied voltage of 100 V, average field strength estimated at 530 V/cm. The dashed line is the calculated steady state concentration profile for average field strength of 530 V/cm. The dotted line is the predicted fluorescence based on local pH [30].

of the channel, but fluorescein's own electrophoretic behavior cannot be ignored. To model fluorescein, values for absorbance, quantum yield, and proton dissociation were used those quoted by Sjoback *et al.* [30]. The pH gradient was assumed to be identical to the gradient determined by p*I* marker focusing, as the field strengths and sample compositions were similar. The resulting focusing (pixel intensities were in the linear range of the camera) agreed with model predictions (Fig. 2b).

3.2 Focusing of amphoteric dyes

Free flow IEF can, in principle, focus anything with a p*I*, regardless of molecular weight. However, the high diffusivity of low-molecular-weight compounds imply that high electric fields are required to observe focusing of lower molecular weight compounds. As a demonstration of the high fields possible with the present design, low-molecular-weight p*I* markers [31–33] and fluorescein were successfully focused in the device.

Fluorescent IEF markers with p*I*'s less than the anode or greater than the cathode gel pK_a were selected, in order to better characterize the interaction between the sample and gel electrode. Figure 3 shows the focusing of a mixture of five different markers: 3.5, 5.1, 7.2, 7.6, and 9.5. As expected, species with p*I*s outside the pH range defined by the anode and cathode pK_a's are driven out of the sample channel and into the corresponding gel sections by electrophoresis. Markers with p*I*'s of 3.5 and 9.5 were focused inside the anode and cathode gels, respectively. In comparison with Kohlheyer *et al.* [2], the increased channel cross-section (50×1000 *vs.* 15×500 μm) reduces the overall resolution, but allows for higher volumetric flow rates (55 *vs*. 20 nL/s) and a greater than 40-fold reduction in hydraulic resistance.

Ampholine 3–10 used in the sample buffer is designed to create a linear pH gradient for IEF applications. Linear regression on the peaks (3.5, 5.1, 7.2, and 7.6) in Fig. 3 (cooled device) yields a linear fit (pH = 5.29×10^{-3}(μm) + 2.94, with R^2 = 0.985). This fit implies that a linear pH gradient does form in the sample channel, but only in the range of 2.9–8.2. The absence of high pH markers and ampholytes leads to the conclusion that EOF is responsible for shifting the focused bands toward the cathode. The asymmetric focusing of the p*I* 5.1 marker, which extends as far as pH 6.4, could be a characteristic of the dye, an impurity, or a degradation product.

For the experiment shown in Fig. 3, a total of 168 mW of electrical power must be removed from the device. Under adiabatic conditions, this would heat 1 μL (the volume of the sample channel) of water at a rate of 40°C/s. In practice, the device was measured (with a thermocouple applied to the glass bottom of the device) to reach temperatures of at least 42°C, raising concerns of Joule heating. At high field strengths, increased Joule heating becomes disruptive to focusing as heat is generated faster than it can be dissipated by the device. Elevated operating temperatures are disruptive to device operation, creating bubbles and increasing the EOF. To prevent the device from overheating, a thermoelectric element was used to cool the top of the device. A cooling module with a water-cooled hot side and connected to the device *via* a silicon heat spreader was fixed to the top of the device. This cooling rate was sufficient to more than compensate for Joule heating in the sample chamber. At excessive cooling rates, condensation formed on the surface of the glass coverslip, reduces the fluorescence signal from the channel. To compare focusing between devices with and without cooling, a second device was operated at the 200 V with the same sample mixture but without external cooling. Without cooling, the best results obtained were relatively broad peaks, with an increased EOF (Fig. 3). Also, the channel was frequently blocked by the formation of bubbles due to dissolved gasses loosing solubility at the elevated liquid temperatures.

In order to test the effects of using Immobilines *versus* an unfunctionalized acrylamide gel, several devices were prepared using a 15% T, 3% C gel in both the anode and cathode regions, but without the addition of the Immobilines. The effect of Immobilines on device performance is shown in Fig. 4. While the steady state results for both gel

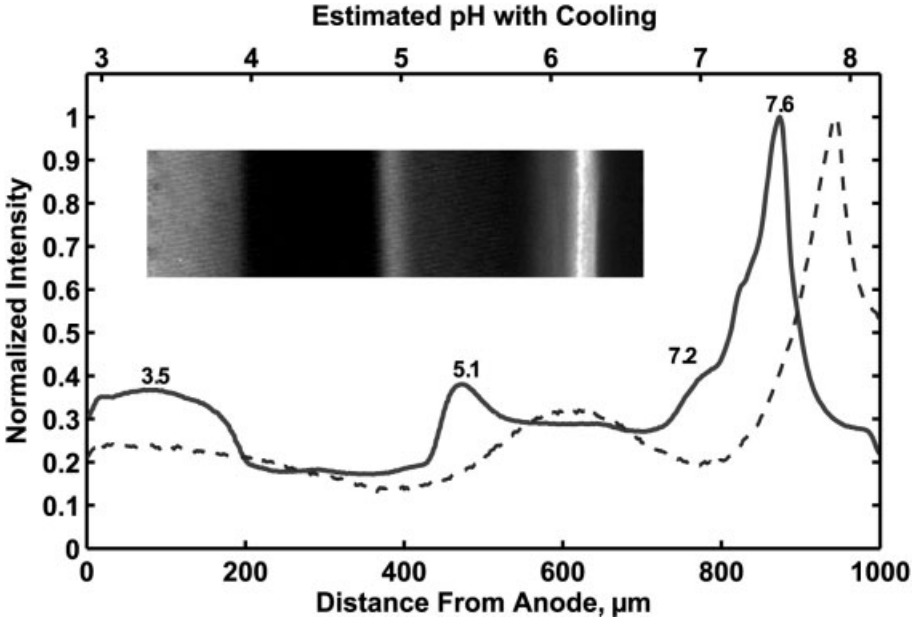

Figure 3. Focusing of IEF markers with cooling (solid line) and without cooling (dashed line). Applied voltage was 200 V with a focusing time of 14 s. Inset: contrast enhanced microscope image with anode to the left, cathode to the right. Markers with p*I*'s of 3.5, 5.1, 7.2, and 7.6 focus within the sample channel. Marker with p*I* 9.5 leaves the channel through the cathode side gel and accumulates in catholyte reservoir. The focusing occurs rapidly with an electric field estimated to be 520 V/cm. The estimated field strength without cooling is 140 V/cm. Both experiments were carried out at 200 V.

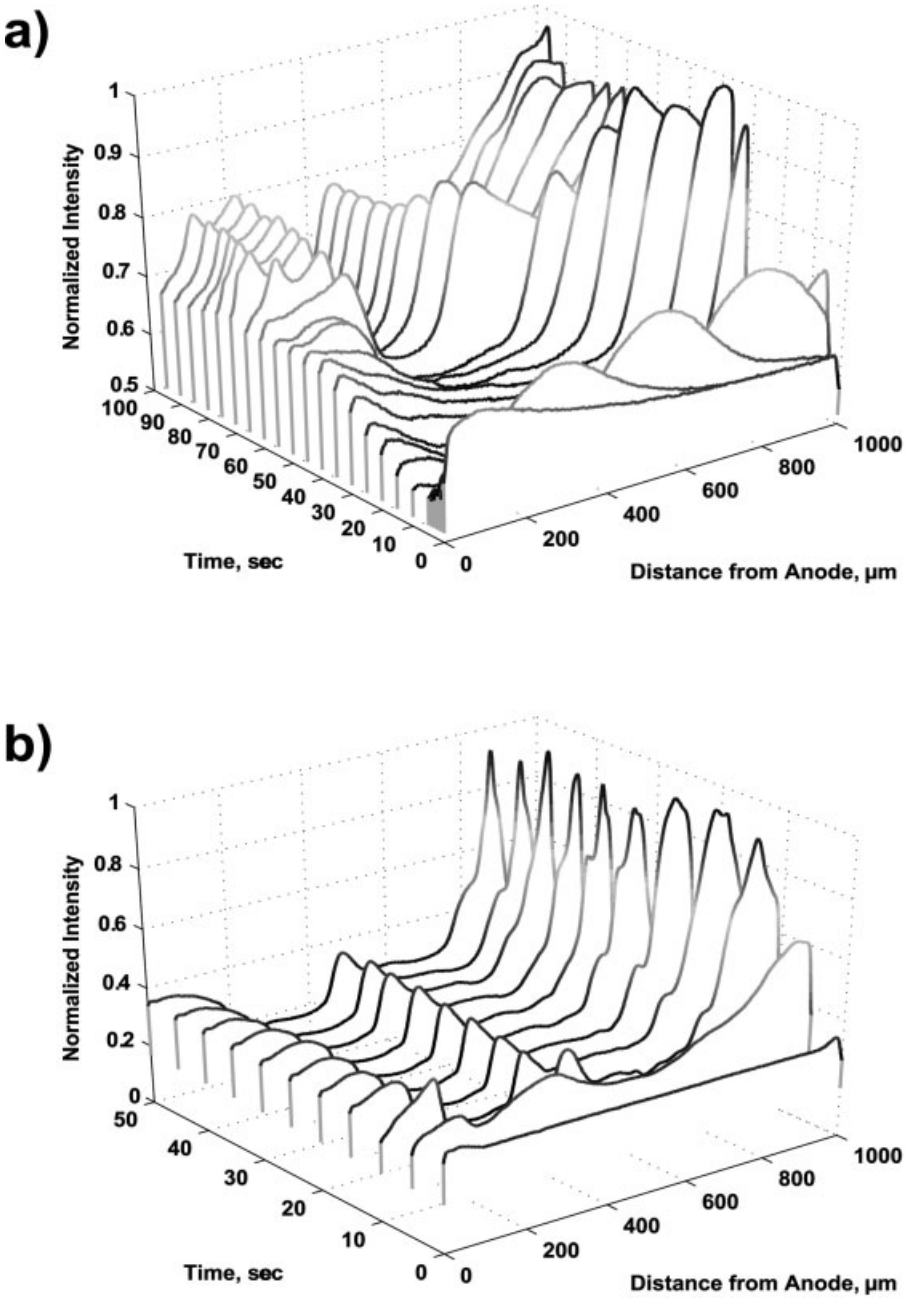

Figure 4. Time evolution of dye focusing with and without functional gels. (a) Time course without immobilized pH groups. Here, plots spaced by 1 s for the first 5 s demonstrate the rapid electrophoresis of the dye mixture into the cathode. Subsequent plots were spaced by 5 s. (b) Time course with immobilized pH groups spaced by 5 s show a decreased time for pH gradient formation.

types were similar, the unfunctionalized gel typically required more than 60 s at 200 V, and 15 min at 50 V to reach a steady state. For comparison, Hagedorn *et al.* [16] observed a 20 min stabilization time for a channel formed from unmodified agarose gel. Because unfunctionalized gels have no buffering capacity, making them less effective for FF-IEF, Kohlheyer *et al.* [2] used buffer side streams with their design. These side streams provide the pH stabilization in lieu of the plain acrylamide gel, which is used simply as a salt bridge.

3.3 Protein separations

An interesting application for free-flow IEF is not only protein focusing, but also focusing of protein complexes. To demonstrate this in micro free-flow IEF, Protein G and mouse IgG were selected. Protein G exhibits a strong avidity for the Fc region in some mammalian Igs, especially mouse IgG. Figure 5 shows the fluorescent intensity of focused Protein G and Protein G–IgG complex at various concentrations of mouse IgG. At increasing con-

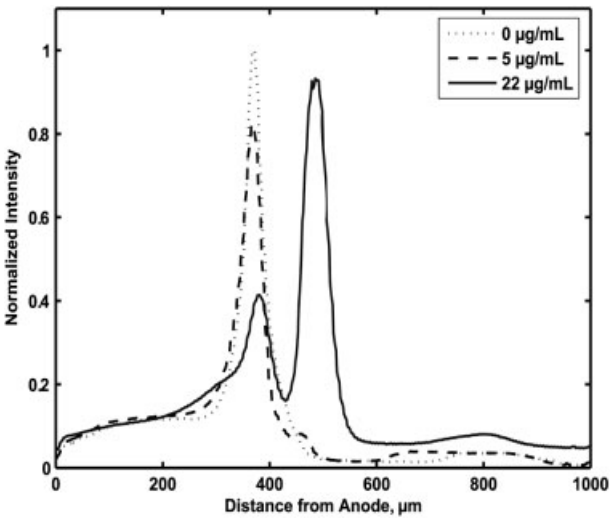

Figure 5. Focusing of Alexa 488-conjugated Protein G at various levels of unlabeled mouse IgG. Plotted are fluorescent intensities normalized to Protein G alone (dotted line). Plots of 5 μg/mL of IgG (dashed line) and 22 μg/mL (solid line) show the focusing of the IgG–Protein G complex. The proteins were focused in less than 20 s with an applied voltage of 30 V; the average electric field is estimated to be approximately 110 V/cm.

centrations of IgG, a second was peak formed and became dominant, indicating that the Protein G–IgG complex had a higher p*I* than Protein G alone. This is consistent with published results for cIEF [34], where Alexa-conjugated Protein G was measured to have a p*I* of 4.2, and the Protein G–IgG complex was observed to focus at a higher p*I*. Over the duration of this experiment (approximately 1 h) the Protein G band was observed to focus on the same point within the device, demonstrating the operational stability of the device over time.

Because of the high concentration of salt in the PBS buffer, the pH range is not expected to be linear over the entire width of the channel. Rather, the linear pH range created by the ampholytes will form in the center of the channel and will be bordered at both pH extremes by dissociated PBS ionic species (*e.g.*, phosphoric acid and potassium hydroxide). These results in the narrower space that the proteins occupy in the sample channel, which is not consistent with the more linear pH profiles in Figs. 2–4. High ionic concentrations at the edges of the sample channel will also decrease the local electric field, reducing resolution near the anode and cathode. However, the results are reproducible from run to run making the high voltage, free flow IEF device a promising tool for separating protein complexes.

4 Concluding remarks

The use of functionalized polyacrylamide as a conductive bridge as well as localized cooling of the sample has been demonstrated as a technique to enhance the performance of micro free flow IEF devices. Electrode isolation permitted the hydrolysis reactions necessary for a high-applied field, while preventing the gaseous hydrolysis products from interfering with the fluid flow. Here, functionalized gels have also been shown to be capable of providing the buffering capacity needed for stable device operation. Incorporation of thermoelectric coolers with the microelectrophoresis device mitigated the Joule heating effects that are problematic at high electric fields. Active cooling leads to more reliable device operation at high voltages. The chemical functionality of the gel, in conjunction with a thermoelectric cooling element enabled rapid separations, without excessive heating or buffer sheath flow.

The placement of these gels is easily defined by PDMS posts made from a relatively low resolution (~20 μm) SU-8 master. These posts eliminate the need for the extra masks and alignment necessary for UV-initiated polymerization. In the fabrication in PDMS, as well the ability to easily cast gels with different functionalities simplifies the fabrication process. Stable operation of the device presented here does not require buffer sheath flow, reducing the experimental complexity as well as setup labor. Also, the open sample channel lowers hydraulic resistance, and can pass large, nonideal samples such as protein aggregates and organelles.

We also report the first application of micro free-flow IEF to focus protein complexes. The separation of free and complexed Protein G demonstrates how these devices may be used as tools for prefractionation or analytical separation of proteins and protein complexes. Nondenaturing separations of protein complexes may prove to be useful tools in elucidating protein complex formation in cellular signaling pathways.

Functionalized polyacrylamide as a conductive bridge could also form the basis for other high-voltage microfluidic separation techniques. Thermal management in microfluidic systems is also a key concern for high voltage applications due to the high energies that must be dissipated. This combination of gel electrical interfaces and local cooling overcomes two of the major barriers to high voltage microfluidics.

We thank the National Institutes of Health (P50-GM68762) for funding; the staff of the MIT Microsystems Technology Laboratories for technical support; John Tolsma (Numerica Technologies) for assistance with Jacobian;

B. K. Shum for assistance with device fabrication; as well as H. Lu, S. Gaudet, J. Kralj, and H. G. Choi for valuable discussions.

5 References

[1] Han, J., Singh, A. K., *J. Chromatogr. A* 2004, *1049*, 205–209.

[2] Kohlheyer, D., Besselink, G. A. J., Schlautmann, S., Schasfoort, R. B. M., *Lab Chip* 2006, *6*, 374–380.

[3] Macounova, K., Cabrera, C. R., Yager, P., *Anal. Chem.* 2001, *73*, 1627–1633.

[4] Song, Y. A., Hsu, S., Stevens, A. L., Han, J. Y., *Anal. Chem.* 2006, *78*, 3528–3536.

[5] Xu, Y., Zhang, C. X., Janasek, D., Manz, A., *Lab Chip* 2003, *3*, 224–227.

[6] Dolník, V., Liu, S. R., Jovanovich, S., *Electrophoresis* 2000, *21*, 41–54.

[7] Giddings, J. C., *Sep. Sci. Technol.* 1983, *18*, 765–773.

[8] Reschiglian, P., Zattoni, A., Roda, B., Michelini, E., Roda, A., *Trends Biotechnol.* 2005, *23*, 475–483.

[9] Lu, H., Gaudet, S., Schmidt, M. A., Jensen, K. F., *Anal. Chem.* 2004, *76*, 5705–5712.

[10] Michel, P. E., Reymond, F., Arnaud, I. L., Josserand, J. *et al.*, *Electrophoresis* 2003, *24*, 3–11.

[11] Ros, A., Faupel, M., Mees, H., van Oostrum, J. *et al.*, *Proteomics* 2002, *2*, 151–156.

[12] Zhang, C. X., Manz, A., *Anal. Chem.* 2003, *75*, 5759–5766.

[13] Raymond, D. E., Manz, A., Widmer, H. M., *Anal. Chem.* 1994, *66*, 2858–2865.

[14] Janasek, D., Schilling, M., Franzke, J., Manz, A., *Anal. Chem.* 2006, *78*, 3815–3819.

[15] Fonslow, B. R., Bowser, M. T., *Anal. Chem.* 2005, *77*, 5706–5710.

[16] Hagedorn, R., Schnelle, T., Muller, T., Scholz, I. *et al.*, *Electrophoresis* 2005, *26*, 2495–2502.

[17] Chein, R. Y., Yang, Y. C., Lin, Y. S., *Electrophoresis* 2006, *27*, 640–649.

[18] Duffy, D. C., McDonald, J. C., Schueller, O. J. A., Whitesides, G. M., *Anal. Chem.* 1998, *70*, 4974–4984.

[19] Xiao, D. Q., Van Le, T., Wirth, M. J., *Anal. Chem.* 2004, *76*, 2055–2061.

[20] Herr, A. E., Singh, A. K., *Anal. Chem.* 2004, *76*, 4727–4733.

[21] Merkel, T. C., Bondar, V. I., Nagai, K., Freeman, B. D., Pinnau, I., *J. Polym. Sci. Part B* 2000, *38*, 415–434.

[22] Zhao, B., Li, Y., Tong, H. L., Zhuo, Y. Q. *et al.*, *Chem. Eng. Sci.* 2005, *60*, 863–868.

[23] Wu, D. P., Luo, Y., Zhou, X. M., Dai, Z. P., Lin, B. C., *Electrophoresis* 2005, *26*, 211–218.

[24] Bier, M., Paulinski, O. A., Mosher, R. A., Saville, D. A., *Science* 1983, *219*, 1281–1287.

[25] Paulinski, O. A., Graham, A., Mosher, R. A., Bier, M., Saville, D. A., *AIChE J.* 1986, *32*, 215–223.

[26] Mosher, R. A., Thormann, W., *Electrophoresis* 2002, *23*, 1803–1814.

[27] Mosher, R. A., Thormann, W., Kuhn, R., Wagner, H., *J.Chromatogr.* 1989, *478*, 39–49.

[28] Mosher, R. A., Gebauer, P., Caslavaska, J., Thormann, W., *Anal. Chem.* 1992, *64*, 2991–2997.

[29] Cannan, R. K., Kibrick, A., Palmer, A. H., *Ann. NY Acad. Sci.* 1941, *41*, 243.

[30] Sjoback, R., Nygren, J., Kubista, M., *Spectrochim. Acta A Mol. Biomol. Spectrosc.* 1995, *51*, L7–L21.

[31] Šlais, K., Friedl, Z., *J. Chromatogr. A* 1994, *661*, 249–256.

[32] Šlais, K., Friedl, Z., *J. Chromatogr. A* 1995, *695*, 113–122.

[33] Horka, M., Willimann, T., Blum, M., Nording, P. *et al.*, *J. Chromatogr. A* 2001, *916*, 65–71.

[34] Tan, W., Fan, Z. H., Qiu, C. X., Ricco, A. J., Gibbons, I., *Electrophoresis* 2002, *23*, 3638–3645.

